Available online at www.sciencedirect.com
SCIENCE DIRECT®
Biochemical Pharmacology 67 (2004) 1363–1372
Biochemical Pharmacology
www.elsevier.com/locate/biochempharm

# Functional characterization of aryl hydrocarbon receptor (zfAHR2) localization and degradation in zebrafish (*Danio rerio*)

Jeannette N. Wentworth, Robert Buzzeo, Richard S. Pollenz*

*Department of Biology, University of South Florida, 4202 E Fowler Ave SCA 110, Tampa, FL 33620-5200, USA*

Received 26 September 2003; accepted 4 December 2003

**Abstract**

The basic-helix-loop-helix/PAS (bHLH/PAS) family of proteins is a group of transcription factors that regulate key pathways during normal development and in the response to stress. The aryl hydrocarbon receptor (AHR) is a member of this family. Recently, *Danio rerio* (zebrafish) has become an important model system in the study of the signal transduction pathway and complements the results seen in mammalian models. However, studies of the AHR protein have been limited by the lack of antibody reagents and thus, little is known concerning the localization and degradation of the zebrafish AHR (zfAHR). In this report, we describe the production and characterization of specific polyclonal antibodies to the zfAHR2 protein and the analysis of AHR-mediated signal transduction in the zebrafish liver cell line (ZFL). The results show that the zfAHR2 is degraded via the 26S proteasome following exposure of cells to β-naphthoflavone (BNF). Interestingly, the time course is slower and the magnitude of zfAHR2 degradation is not as great as seen for the mammalian AHR. Studies also show that the zfAHR2 is rapidly degraded in a ligand-independent manner by exposure of cells to geldanamycin (GA) to levels consistent with mammalian AHR. Finally, immunohistochemical staining of the ZFL cells suggest that the unliganded AHR resides in both the cytoplasm and nucleus and undergoes active nucleocytoplasmic shuttling in the absence of ligand. These results suggest that there is conservation of function between fish and mammals with respect to ligand-dependent and -independent degradation of the AHR and that the zfAHR2 is degraded via the 26S proteasome.


*Keywords:* Aryl hydrocarbon receptor; Zebrafish; TCDD; ZFL cell line; Protein degradation; 26S proteasome

## 1. Introduction

*Danio rerio* (zebrafish) has become an important model system in the study of development and signal transduction pathways. Recent studies indicate that zebrafish show sensitivity to TCDD during development as well as exhibit disruption of erythropoiesis [1], altered regional blood flow and impaired lower jaw development [2], apoptosis and local circulation failure in the dorsal midbrain [3] and edema, retarded development and craniofacial abnormalities [4]. These biological endpoints to TCDD exposure correlate well with those from mammalian systems and recent studies using morpholino-oligonucleotide knock down of zfAHR2 expression have implicated the zfAHR2 in mediating many of these biological effects [5].

Currently, complete cDNAs for the AHR have been characterized from numerous species of fish including rainbow trout and zebrafish [6–8]. The most striking finding is that there appears to be two classes of AHR genes in many of the fish species (termed AHR1 and AHR2) that exist due to a genomic duplication event that took place in early vertebrate evolution. Amino acid sequence comparison shows that the AHR1 and AHR2 share the greatest similarity within the NH-terminal region of the protein that contains the DNA binding basic region, helix-loop-helix (HLH), nuclear localization signal (NLS) and PAS domains [6,7]. In spite of the sequence similarity, the zfAHR2 protein exhibits higher affinity for TCDD than the zfAHR1 protein and shows a

* Corresponding author. Tel.: +1-813-974-1596; fax: +1-813-974-3263.
*E-mail address:* pollenz@chuma1.cas.usf.edu (R.S. Pollenz).

*Abbreviations:* AHR, aryl hydrocarbon receptor; zfAHR2, zebrafish AHR2; bHLH, basic-helix-loop-helix; ARNT, aryl hydrocarbon receptor nuclear translocator; TCDD, 2,3,7,8-tetrachlorodibenzo-*p*-dioxin; PAS, PER-ARNT-SIM; HIF, hypoxia-inducible factor; BNF, β-naphthoflavone; SDS–PAGE, sodium dodecyl sulfate polyacrylamide gel electrophoresis; GAR-HRP, goat anti-rabbit horseradish peroxidase; PBS, phosphate-buffered saline; TBS, Tris-buffered saline; TTBS, Tris-buffered saline with Tween 20; BSA, bovine serum albumin; TBE, Tris boric acid EDTA; DMEM, Dulbecco's minimum essential media; FBS, fetal bovine serum; PCR, polymerase chain reaction; SDS, sodium dodecyl sulfate; RL, reticulocyte lysate; PI, pre-immune IgG.

0006-2952/$ – see front matter © 2003 Elsevier Inc. All rights reserved.
doi:10.1016/j.bcp.2003.12.002

far greater propensity for inducing dioxin responsive reporter genes in recombinant cell culture systems [7]. In fact, zfAHR1 appears to lack ligand binding so its role in AHR-mediated signaling events is unclear and will require detailed analysis at the protein level.

The current model of AHR-mediated signal transduction has been generated based on mammalian models. The model proposes that the AHR is in an inactive conformation, usually within the cytoplasm of cells, although it may be shuttling between the nucleus and cytoplasm [9]. Regardless of its subcellular location, the AHR is held in an inactive state because it is complexed with hsp90 and immunophilin-like proteins [10]. Following binding to ligands typified by TCDD, the AHR protein complex becomes "transformed" and the entire AHR hsp90 immunophilin complex is translocated or retained within the nucleus [10–12]. Once in the nucleus, the liganded AHR appears to have several fates. It first has the potential to dimerize with the ARNT protein and then associate with a xenobiotic response element (XRE), to provide regulatory control to genes in a positive or negative manner [13]. However, the AHR is also a substrate for the 26S proteasome [14] and can be targeted for degradation either within the nucleus [15] or within the cytoplasm following nuclear export [16–18]. Importantly, reductions in the level of AHR protein can impact both cell growth in culture [19] and normal developmental processes *in vivo* [20–24]. Indeed, some of the phenotypes observed in AHR knock out mice (AHRKO) are similar to those reported in TCDD-treated animals. For example, TCDD-like effects on reproduction and ovary development are prominently observed in AHRKO mice that have *not* been exposed to TCDD [24–27]. These findings strongly correlate the level of the AHR protein to growth and development and support the hypothesis that unprogrammed reductions in AHR protein (through exogenous ligand exposure) may disrupt endogenous signaling pathways that influence transcriptional events involved in growth and differentiation.

To be able to investigate the interaction of the zfAHR isoforms with other proteins and characterize their degradation, it is essential to have specific antibodies capable of detecting these proteins both *in vivo* and *in vitro*. In this report, we describe the production and characterization of specific polyclonal antibodies to the zfAHR2 protein and the analysis of AHR-mediated signal transduction in the zebrafish liver (ZFL) cell line. The results show that the zfAHR2 is degraded via the 26S proteasome following exposure of cells to BNF although the time course and magnitude of the degradation events are different than those observed in mammalian cell lines. In addition, the zfAHR2 can be degraded in a ligand-independent manner by exposure of cells to geldanamycin (GA). Finally, immunohistochemical staining of the ZFL cells suggest that the unliganded AHR resides in both the cytoplasm and nucleus and appears to undergo active nucleocytoplasmic shuttling in the absence of ligand.

## 2. Materials and methods

### 2.1. Antibodies and reagents

Specific antibodies against the mouse AHR (A-1A) are identical to those described previously [28]. For Western blot analysis goat anti-rabbit antibodies conjugated to horseradish peroxidase (GAR-HRP) were utilized. For immunohistochemical studies, goat anti-rabbit IgG conjugated to rhodamine (GAR-RHO) was used. Both of these reagents were purchased from Jackson Immunoresearch. Polyclonal rabbit β-actin antibodies, leptomycin B and BNF were purchased from Sigma-Aldrich. MG-132 was purchased from Calbiochem.

### 2.2. Buffers

PBS is 0.8% NaCl, 0.02% KCl, 0.14% $Na_2HPO_4$, 0.02% $KH_2PO_4$, pH 7.4. 2X gel sample buffer is 125 mM Tris, pH 6.8, 4% SDS, 25% glycerol, 4 mM EDTA, 20 mM DTT, 0.005% bromophenol blue. TBS is 50 mM Tris, 150 mM NaCl, pH 7.5. TTBS is 50 mM Tris, 0.2% Tween 20, 150 mM NaCl, pH 7.5. TTBS+ is 50 mM Tris, 0.5% Tween 20, 300 mM NaCl, pH 7.5. BLOTTO is 5% dry milk in TTBS. 2X lysis buffer is 50 mM Hepes, pH 7.4, 40 mM sodium molybdate, 10 mM EGTA, 6 mM $MgCl_2$, 20% glycerol.

### 2.3. Cells and growth conditions

Zebrafish liver cells were purchased from American Type Culture Collection. Type I Hepa-1 variants (LA-I) were a generous gift from Dr. Jim Whitlock, Jr. (Department of Pharmacology, Stanford University). LA-I cells were propagated at 37° in DMEM media containing 5% FBS. ZFL cells were propagated at 28° in a 0.5:0.35:0.15 mixture of L-15/DMEM/Ham-F12 supplemented with bovine insulin (5 mg/L), mouse epidermal growth factor (10 μg/L) and heat inactivated FBS (5%) as specified by supplier. All cells were passaged at 1 week intervals and used in experiments during a 2-month period.

### 2.4. Construction of bacterial expression vectors, purification of zfAHR2 fusion protein and affinity purification of serum

Full-length zfAHR2 cDNA was a generous gift from Robert Tanguay (University of Oregon, OR). To construct the zfAHR2 histidine fusion vector, oligonucleotide primers were used to amplify the region of zfAHR2 that spanned amino acids 816–1027. The DNA fragment was then ligated into pQE8 (Qiagen) to generate pQE8-zfAHR2 and transformed into the M15 strain of *Escherichia coli*. Cells containing the pQE8-zfAHR2 plasmid were propagated to log phase and then incubated for 6 hr at 37° in the presence of isopropyl-β-D-thiogalactopyranoside

(1 mM). Pelleted cells were disrupted by sonication, and inclusion bodies pelleted and dissolved in 6 M guanidine HCl. Histidine fusion proteins were then purified on nickel-agarose beads under denaturing conditions as detailed by the manufacturer (Qiagen). The purified protein was then resolved on 12% polyacrylamide gels, lightly stained with coomassie dye and the bands excised. All antigen injections and bleeding were carried out through Sigma-Genosys. Affinity purification of specific antibodies to the zfAHR2 was carried out as previously detailed [28–30].

### 2.5. In vitro expression of protein

Recombinant protein was produced from expression constructs using the TNT™ Coupled Rabbit Reticulocyte Lysate Kit essentially as detailed by the manufacturer. Upon completion of the 90 min reaction, samples were either combined with an equal volume of 2X gel sample buffer and boiled for 5 min, or stored at −80° for use in functional studies.

### 2.6. Production of total cell lysates

Cells were harvested from plates by trypsinization and then washed twice in ice cold PBS. Total cell lysates for Western blot analysis were prepared by sonicating cell pellets in 50–100 μL 2X lysis buffer containing 0.5% NP-40 and then adding an equal volume of 2X gel sample buffer and boiling for 5 min as detailed previously [28–30]. Protein concentrations were determined by the Coomassie Blue Plus assay using BSA as the standard. All samples were stored at −20° prior to SDS–PAGE analysis.

### 2.7. Western blot analysis and quantification of protein

Protein samples were resolved by denaturing electrophoresis on discontinuous polyacrylamide slab gels (SDS–PAGE) and were electrophoretically transferred to nitrocellulose. Immunochemical staining was carried out with varying concentrations of primary antibody (see text and figure legends) in BLOTTO buffer supplemented with D,L-histidine (20 mM) for 1–2 hr at 22°. Blots were washed with five changes of TTBS+ for a total of 50 min. The blot was then incubated in BLOTTO buffer containing a 1:12,000 dilution of GAR-HRP for 1 hr at 22° and washed in five changes of TTBS+ as above. Prior to detection, the blots were washed in PBS for 5 min. Bands were visualized with the enhanced chemiluminescence (ECL) kit as specified by the manufacturer. Multiple exposures of each set of samples were produced. The relative concentration of target protein was determined by computer analysis of the autoradiographs and normalization to the internal standard (actin) as detailed previously [28,30–32]. Each experiment was repeated at least three times.

### 2.8. Transient transfection of LA-I cells

LA-1 cells were seeded at $1 \times 10^6$ cells/well onto 35 mm dishes and propagated overnight. A cocktail containing 4 μg zfAHR2 expression vector and 60 μL LipofectAMINE™ (Gibco) transfection reagent was prepared in 2.6 mL of cell culture media. This volume was sufficient for transfecting 12 dishes with the exact same solution of DNA and the transfection was carried out according to the manufacturer's instructions. After a 6–8 hr transfection period, cells were fed with fresh media containing FBS and allowed to recover for 16 hr prior to experimental treatments. Cells were then harvested from plates and processed for SDS–PAGE as detailed above.

### 2.9. Immunofluorescence staining, microscopy and quantification of nuclear fluorescence

All immunohistochemical procedures (cell plating, fixation, staining and photography) were carried out as previously described [28,29] and are detailed in the figure legends. Cells were observed on an Olympus microscope using the 568 nm filter. On average, 15–20 fields (5–20 cells each) were evaluated on each coverslip and 3–4 fields were digitally photographed to generate the raw data. Fluorescence intensity was quantified in the nucleus of cells by NIH Image 1.55 software. Briefly, digital images taken from cells stained for identical time frames in the same staining solutions, were converted to negatives in Adobe Photoshop 6.0. The pixel density of the nucleus (equal to the relative intensity of the fluorescent signal) was then quantified in NIH Image using a defined size area that was held constant for all cells examined. On average 40–60 cells were evaluated for each treatment group and the values expressed as mean ± SE. Experiments were repeated at least two times.

### 2.10. Statistics

For all calculated values, significance was determined using a two-way ANOVA. All statistical analysis was performed using the InStat program (GraphPad). Results are presented as mean ± SE.

## 3. Results and discussion

### 3.1. Generation and characterization of antibodies against zfAHR2

Previous studies from this lab have utilized bacterial expressed histidine fusion proteins to the NH-terminal 400 amino acids of the murine AHR to produce highly specific antibodies termed A-1 and A-1A [28,29]. The homology between zfAHR isoforms and the mAHR is approximately 70% in this region (Fig. 1A), yet the mAHR A-1A

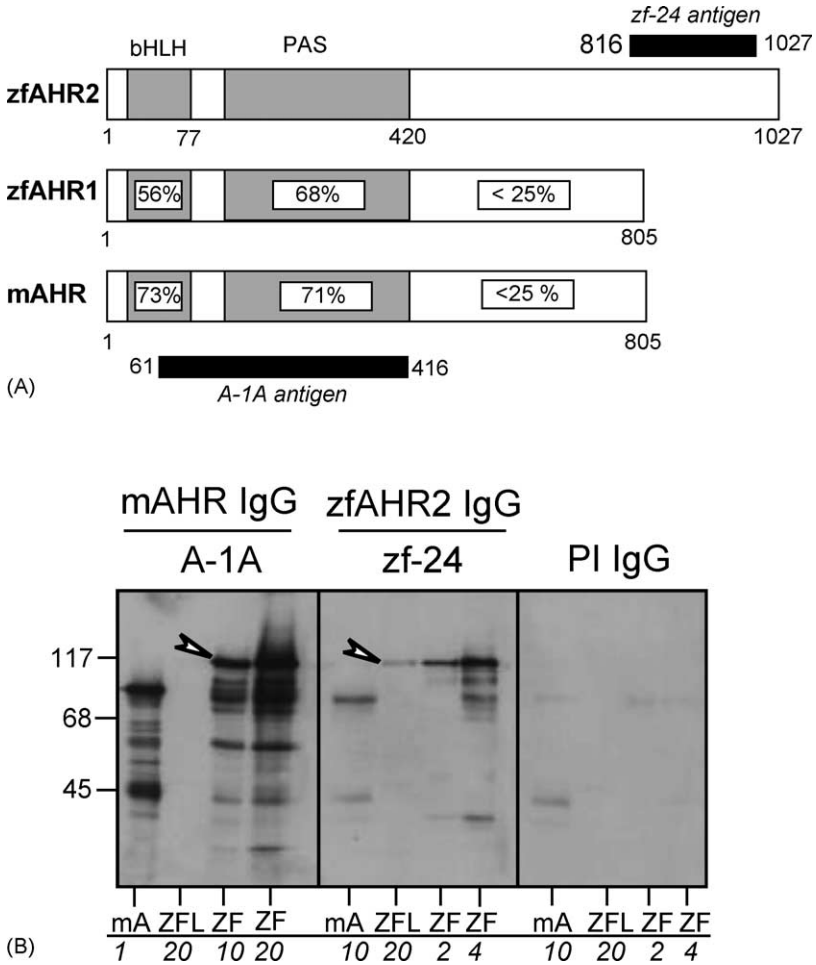


Fig. 1. Generation and specificity of the zf-24 antibody. (A) Schematic of zfAHR1, zfAHR2 and mAHR domains. Numbers in boxes indicate the percentage of amino acid identity in the shaded region. Black bars indicate the region used to generate the A-1A or zf-24 antibodies. Numbers under each receptor indicate amino acids. bHLH, basic-helix-loop-helix; PAS, PER-ARNT-SIM homology region. (B) Western blots. The indicated samples were resolved by SDS–PAGE and analyzed by Western blotting using 1 μg/mL A-1A, zf-24 or pre-immune (PI) IgG, followed by GAR-HRP (1:12,000). The molecular mass of standard proteins is indicated on the left in kDa. mA, *in vitro* expressed mAHR; ZF, *in vitro* expressed zfAHR2; ZFL, 20 μg ZFL total cell lysate. The number under each lane indicates the amount of protein loaded in micrograms (μg). The arrowhead indicates the 113 kDa zfAHR2 protein band.

antibodies show reduced sensitivity to piscine AHR on Western blots and have not been useful to detect endogenous AHR in any fish species (unpublished results). For example, the A1-A antibody detects the *in vitro* expressed mAHR in as little as 1 μg reticulocyte lysate (RL), yet requires loading of 10–20 times more RL (10–20 μg) to detect a band corresponding to the appropriate molecular mass of the zfAHR2 (arrowhead Fig. 1B). Previous studies have established that each microliter of RL contains 5–10 ng of *in vitro* expressed target protein [28,29]. In addition, the A-1A antibody does not detect protein bands that correspond to the appropriate molecular mass of the zfAHR2 in 20 μg of total cell lysate prepared from the ZFL cell line (first panel in Fig. 1B). Thus, it was necessary to produce new antibodies that would show high levels of sensitivity to zfAHR2. Since, the deduced amino acid sequences of the zfAHR1 and zfAHR2 proteins show significant identity in the NH-terminal region (Fig. 1A), it was desirable to produce an antibody that would be specific to only the zfAHR2 protein. Thus, a histidine fusion protein was expressed and purified from bacteria that contained the COOH-terminal 211 amino acids of the zfAHR2 coding sequence (amino acids 816–1027). This region of the zfAHR2 shares 25% identity with the zfAHR1 protein or mAHR (Fig. 1A) and should have minimal cross-reactivity with these proteins. Following injection in rabbits, IgG specific to the zfAHR2 was affinity purified and its specificity and sensitivity evaluated by Western blotting of *in vitro* expressed protein and ZFL total cell lysates. The zfAHR2 antibody was termed zf-24.

Figure 1B shows that zf-24 IgG reacts with a protein that corresponds to the appropriate molecular mass (113 kDa) of the zfAHR2 (arrowhead). Importantly, 1 μg/mL of the zf-24 IgG could detect *in vitro* expressed zfAHR2 in as little as 2 μg of RL. As expected, zf-24 IgG does not react with *in vitro* expressed mAHR even when 10 μg of RL is loaded. Importantly, the zf-24 IgG detects a single protein band in 20 μg of total cell lysate derived from the ZFL cell line and the band co-migrates with the *in vitro* expressed zfAHR2 (arrowhead). No other bands approaching the

intensity of the zfAHR2 were observed in the ZFL total cell lysate and the lower molecular mass bands observed in the RL lanes likely represent partially degraded zfAHR2 that occur as a consequence of the *in vitro* synthesis. The specificity of the zf-24 IgG is further demonstrated by the lack of reactivity of pre-immune (PI) IgG to ZFL total cell lysate and to the RL containing *in vitro* expressed zfAHR2. To further characterize the zf-24 antibody and to validate its utility for quantitative Western blotting, graded concentrations of RL containing *in vitro* expressed zfAHR2 were resolved by SDS–PAGE, blotted to nitrocellulose and stained. The resulting protein bands were quantified by computer densitometry as detailed in Section 2 and the linearity of the antibody's reactivity determined by regression analysis. The results in Fig. 2 show that the zf-24 antibody can accurately detect the zfAHR2 over a 5-fold range of protein concentration and thus, can be used for quantitative analysis of zfAHR2 protein in cells and tissues.

### 3.2. Detection of zfAHR2 in transfected murine cells

The LA-1 cell line has been a powerful tool for evaluating AHR function *in vivo* [17–19]. Studies were initiated to (i) determine whether the zf-24 antibody could detect zfAHR2 protein when LA-I cells were transiently transfected with zfAHR2 expression vectors, (ii) whether the zfAHR2 protein would be degraded following exposure of cells to BNF or GA and (iii) to further characterize the specificity of the zf-24 antibody. LA-1 cells were transfected with zfAHR2 expression vectors as detailed in Section 2 and then treated with BNF (5 μM) for 7 hr or GA (100 nM) for 2 hr. Following each treatment cells were harvested, and total cell lysates evaluated by Western blotting. Figure 3 shows a representative experiment. The zf-24 antibody does not react with any proteins in the mock transfected LA-I control cells while a protein migrating at approximately 113 kDa is clearly detected in the cells transfected with the zfAHR2 expression vector. Importantly, the level of zfAHR2 protein is reduced by 42% following 7 hr of BNF exposure and by >70% following 2 hr of GA exposure. This level of degradation is consistent with previous studies that have evaluated the degradation of the mAHR in transiently transfected cells ([16,17], unpublished results), and provide the first evidence that ligand-dependent and -independent degradation of the AHR are events that are conserved between zebrafish and mammals.

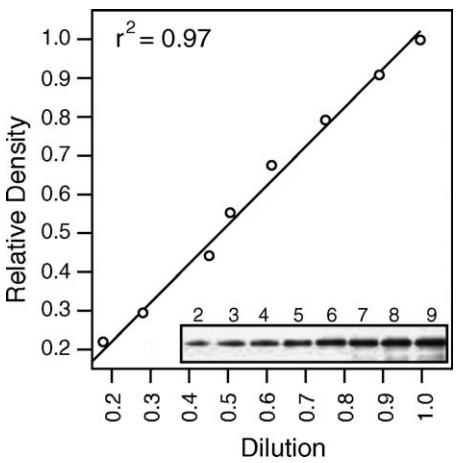


Fig. 2. Linearity of zf-24 antibody. zfAHR2 protein was expressed in RL and 2–9 μL resolved by SDS–PAGE and blotted. The blot was then stained using 1 μg/mL zf-24 IgG followed by GAR-HRP (1:12,000) and quantified by computer densitometry. The relative density of each sample was plotted against the dilution and regression analysis performed using GraphPad Software. Inset is the blot of zfAHR2 with each number representing the loading in μL.

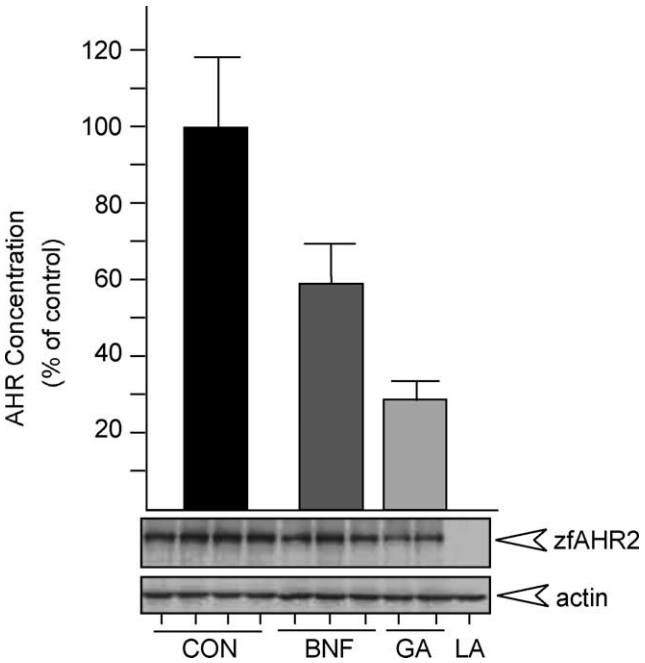


Fig. 3. Expression of zfAHR2 in murine Hepa-1 cells. zfAHR2 expression vectors were transfected into LA-I Hepa-1 cells. Twenty-four hours later, cells were treated with $me_2SO$ (0.01%), BNF (5 μM) for 7 hr or GA (100 nM) for 2 hr. Total cell lysates were prepared, equal amounts resolved by SDS–PAGE and Western blotting performed using 1 μg/mL zf-24 IgG and anti-actin (1:1000) followed by GAR-HRP (1:12,000). zfAHR2 and actin bands were quantified by computer densitometry and the level of zfAHR2 normalized to the level of actin. Data are expressed as the percent of control. Bars represent the mean ± SE except the GA samples that represent the mean and range. LA, LA-1 hepa-1 cells that were mock transfected without zfAHR2 cDNA.

### 3.3. zfAHR2 is degraded via the 26S proteasome following ligand binding

To evaluate the degradation of the endogenous zfAHR2, several experiments were carried out in the ZFL cell line. The ZFL line was derived from zebrafish liver, and has been shown to express various CYP enzymes including CYP1A [33–35]. ZFL cells were propagated to 75% confluence and treated with 5 μM BNF for 0–24 hr. Total cell lysates were then prepared and the level of zfAHR2 protein

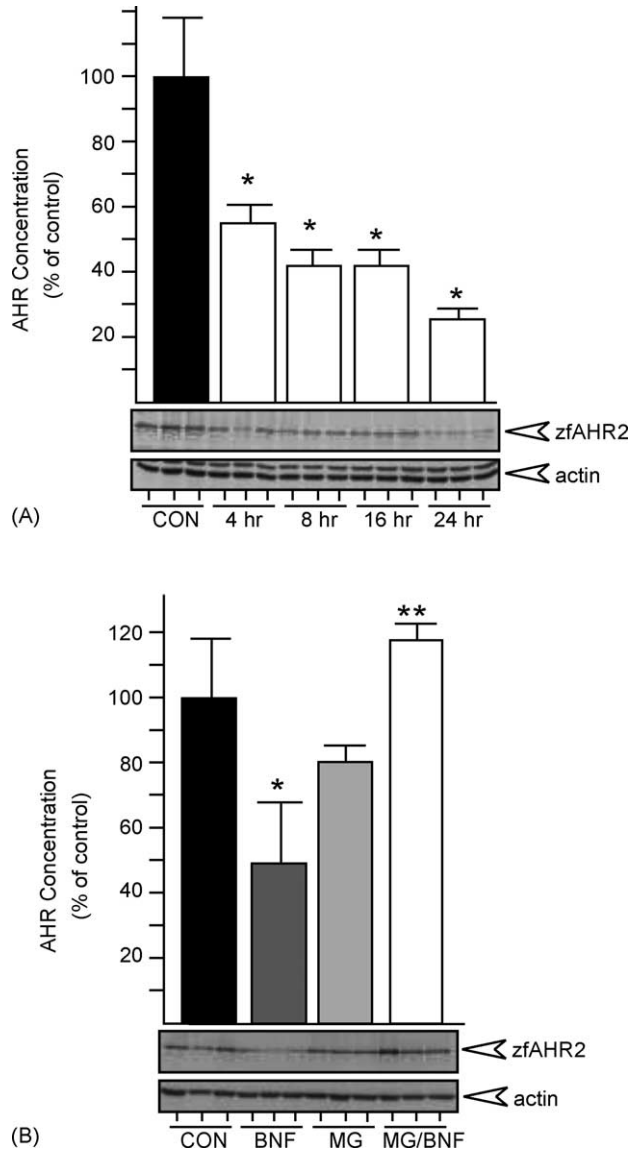


Fig. 4. BNF-mediated degradation of zfAHR2 in ZFL cells. (A) ZFL cells were treated with $me_2SO$ (0.01%) for 24 hr or BNF (5 μM) for 4, 8, 16 or 24 hr. Total cell lysates were prepared, equal amounts resolved by SDS–PAGE and Western blotting performed using 1 μg/mL zf-24 IgG and anti-actin (1:500) followed by GAR-HRP (1:12,000). zfAHR2 and actin bands were quantified by computer densitometry and the level of zfAHR2 normalized to the level of actin. Data are expressed as the percent of control. Bars represent the mean ± SE of three samples. *: statistically different from control ($P \leq 0.05$). (B) ZFL cells were treated with 0.01% $me_2SO$ (CON) for 6 hrs, BNF (5 μM) for 4 hr, 10 μM MG-132 (MG) for 6 hr, or 10 μM MG-132 for 2 hr followed by BNF (5 μM) for an additional 4 hr (MG/BNF). Total cell lysates were prepared and analyzed by Western blotting as detailed in (A). Bars represent the mean ± SE of three samples *: statistically different from control ($P \leq 0.05$); **: statistically different from BNF ($P \leq 0.05$).

determined by quantitative Western blotting. A representative experiment is shown in Fig. 4A. As observed in the transiently transfected LA-1 cells, the zfAHR2 is degraded following exposure to BNF. The level of zfAHR2 protein is reduced by 45% after 4 hr exposure, and shows a reduction of >70% by 24 hr. Thus, as observed in mammalian cells, the endogenous zfAHR2 is degraded following ligand exposure.

Previous studies from this and other laboratories have shown that the mammalian AHR is degraded via the 26S proteasome [16,17,36,37]. To determine if degradation in the ZFL cells were occurring through a similar pathway, ZFL cells were treated with the proteasome inhibitor MG-132 for 2 hr, followed by BNF for an additional 4 hr. Total cell lysates were then prepared and the level of zfAHR2 protein determined by quantitative Western blotting. A representative experiment is shown in Fig. 4B. As observed in Fig. 4A, the zfAHR2 was reduced by approximately 50% following 4 hr of BNF exposure. In contrast, pre-treatment of the cells with MG-132, completely blocked the BNF-mediated degradation of the zfAHR2. Similar results were obtained when lactacystin was used to inhibit proteasome function (data not shown). These results suggest that the zfAHR2 is degraded through the 26S proteasome as observed with mammalian AHRs. However, while the degradation pathway may be similar, the *time course* and overall *level* of zfAHR2 protein degradation is different than that observed in mammalian cells. In mammalian cells, the ligand-mediated degradation of the AHR generally reaches its maximal level within 4 hr of exposure and the magnitude of degradation can reach up to 95% of the endogenous AHR [14–18,36]. Thus, the degradation time course in the ZFL cells was slower (showing maximal levels of degradation at 24 hr) and not as robust (maximal levels of degradation are approximately 70%) as observed in various mammalian cell culture lines. At present, the molecular basis of these differences are not clear but may be due to the lower incubation temperature of the ZFL cells (28.5° vs. 37.5° for mammalian cells), differences in the 26S proteasome between fish and mammals or differences in the location of lysine residues in the zfAHR2 compared to mammalian AHRs.

### 3.4. *zfAHR2 is degraded following exposure to geldanamycin*

GA is a benzoquinone ansamycin that directly associates with ATP/ADP binding site of hsp90 protein [38], and can disrupt the formation of heterocomplexes such as hsp90-pp60v-src [39] and Raf-1/hsp90 [40]. Treatment of both human HeLa and mouse Hepa-1 cells with GA results in dramatic reductions in the level of endogenous AHR protein within 2 hr of exposure in a dose- and time-dependent manner [15,18,41,42]. Thus, it has been hypothesized that loss of chaperone proteins or changes in the conformation of the AHR·hsp90 complex may play a key role in the stability and subcellular localization of the AHR and its recognition by the 26S proteasome.

ZFL cells were propagated to 75% confluence and treated with 100 nM GA for 0–180 min. Total cell lysates were then prepared and the level of zfAHR2 protein determined by quantitative Western blotting. A representative

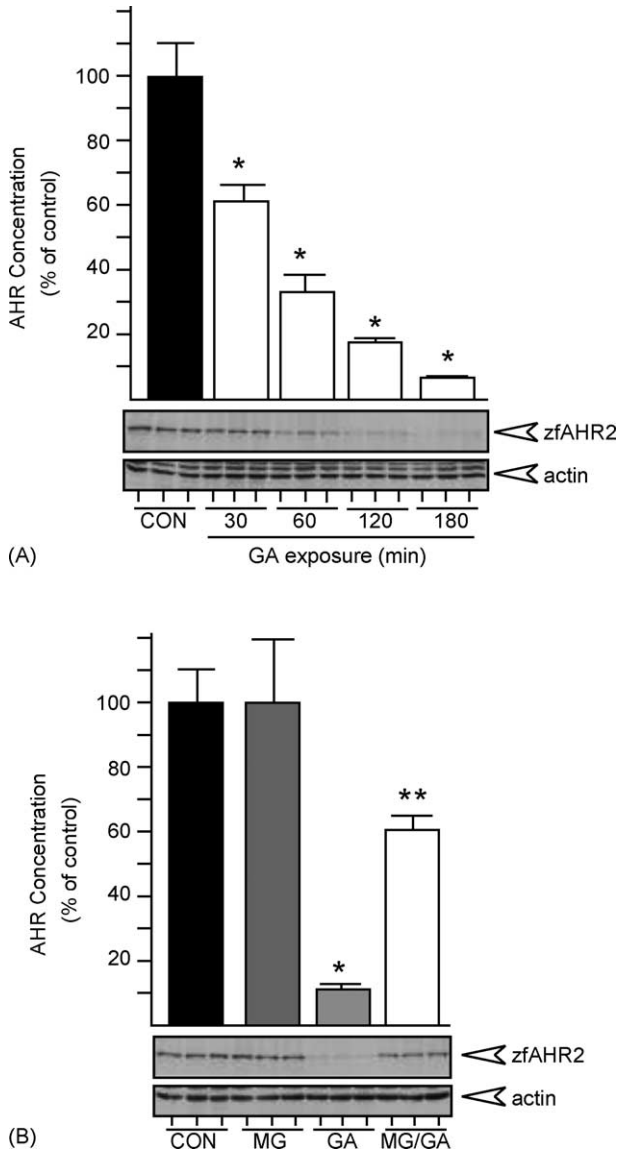


Fig. 5. GA-mediated degradation of zfAHR2 in ZFL cells. (A) ZFL cells were treated with $me_2SO$ (0.01%) for 180 min or GA (100 nM) for 30, 60, 90 or 180 min. Total cell lysates were prepared, equal amounts resolved by SDS–PAGE and Western blotting performed using 1 μg/mL zf-24 IgG and anti-actin (1:500) followed by GAR-HRP (1:12,000). zfAHR2 and actin bands were quantified by computer densitometry and the level of zfAHR2 normalized to the level of actin. Data are expressed as the percent of control. Bars represent the mean ± SE of three samples. *: statistically different from control ($P \leq 0.05$). (B) ZFL cells were treated with 0.01% $me_2SO$ (CON) for 4 hr, GA (100 nM) for 2 hr, 10 μM MG-132 (MG) for 4 hr, or 10 μM MG-132 for 2 hr followed by GA (100 nM) for an additional 2 hr (MG/GA). Total cell lysates were prepared and analyzed by Western blotting as detailed in (A). Bars represent the mean ± SE of three samples. *: statistically different from control ($P \leq 0.05$); **: statistically different from control ($P \leq 0.05$) and GA ($P \leq 0.05$).

experiment is shown in Fig. 5A. The level of zfAHR2 protein was rapidly degraded during the experimental time course and became <10% of the control level after 180 min. When ZFL cells were pretreated with MG-132 for 2 hr and then exposed to GA for an additional 2 hr, the level of GA-mediated zfAHR2 degradation was dramatically reduced (Fig. 5B). In contrast to the ligand-dependant degradation detailed above, the time course and magnitude of the GA-mediated degradation in ZFL cells is consistent with results observed in mammalian cells [15,18,41,42]. The differences between GA and ligand-mediated degradation may be due to fact that GA produces a systemic effect on all hsp90 and does not affect the zfAHR2 directly (i.e. it associates with the hsp90). In addition, the degradation mediated by GA exposure may utilize a different domain of the AHR that recognized following ligand binding (data not shown). Importantly, this data suggest that differences in the incubation temperature of the ZFL cells or in the functioning of the 26S proteasome are unlikely to contribute to the reduced level of degradation observed during ligand exposure.

### 3.5. Subcellular localization of zfAHR2 in ZFL cells

Having established that the zf-24 antibodies could detect the endogenous zfAHR2 protein in total cell lysates, it was of interest to evaluate the subcellular location of the zfAHR2 in cells and the specificity of the zf-24 antibody for immunohistochemical staining. For these studies the ZFL cells were propagated on glass cover slips, treated as detailed below and then fixed and stained as described in Section 2. Figure 6 shows the digital images from a representative experiment and the relative intensity of the nuclear fluorescence of the ZFL cells is presented in Table 1. The distribution of the zfAHR2 in untreated (control) cells appears to be both nuclear and cytoplasmic. However, when the cells were treated with BNF for 2 hr prior to fixation, the intensity of the nuclear staining increased nearly 2-fold with a concomitant reduction in the level of cytoplasmic staining. Since the ZFL cells are rather small, larger images from representative panels are presented at the bottom of Fig. 6 and the change in the subcellular location of the zfAHR2 can be clearly observed. The change in the staining pattern is consistent with a ligand-induced translocation of the cytoplasmic zfAHR2 to the nucleus of the cells as has been observed in several mammalian cell lines [15,18,29]. Importantly, treatment of ZFL cells with BNF for 16 hr resulted in a significant decrease in the intensity of the nuclear staining,

Table 1
Relative density of nuclear fluorescence

| Treatment | Time (hr) | N | Relative nuclear density | Percent of BNF 2 hr |
|---|---|---|---|---|
| Control | – | 47 | 57 ± 32 | 49 |
| BNF | 2 | 52 | 116 ± 32[a] | 100 |
| BNF | 16 | 55 | 62 ± 8.3[b] | 53 |
| LMB | 4 | 48 | 114 ± 28[a] | 100 |
| GA | 2 | 59 | 37 ± 32[b] | 31 |

The pixel density of the nucleus was determined as indicated in Section 2. Values indicate the mean ± SE for the number of samples indicated.
[a] Statistically different from control ($P \leq 0.05$).
[b] Statistically different from BNF 2 hr ($P \leq 0.05$).

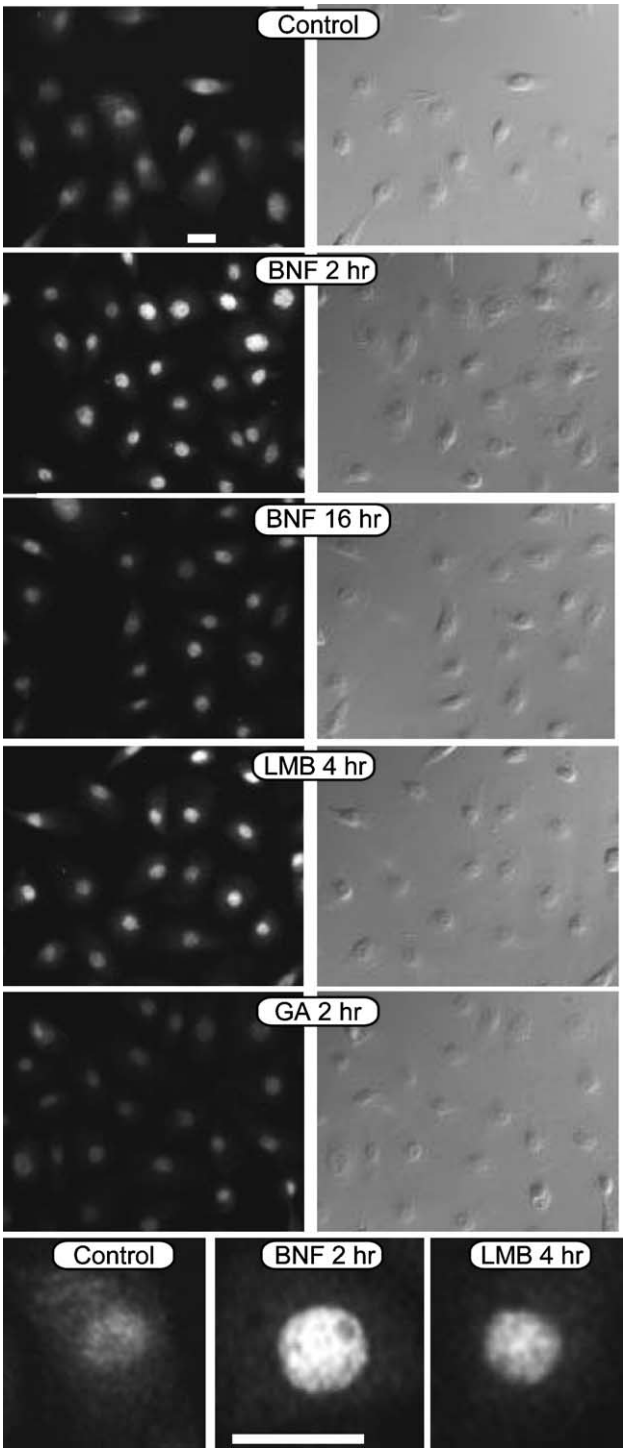


Fig. 6. Subcellular localization of zfAHR2 in ZFL cells. ZFL cells were grown on glass coverslips for 48 hr and then treated with 0.01% $me_2SO$ (CON) for 16 hr, BNF (5 μM) for 2 and 16 hr, 100 nM GA for 2 hr (GA), or 10 nM LMB for 4 hr (LMB). Following treatments, cells were fixed and stained with the identical solution of 1 μg/mL zf-24 IgG followed by GAR-RHO (1:400). Photos on left are fluorescence images while photos on right are Nomarski images. All photos represent identical exposure times. Images on the bottom are larger images of single cells from the control, BNF 2 hr and LMB 4 hr fields. Bar in controls = 2 μm.

consistent with the 50% degradation of the zfAHR2 protein observed in Fig. 4. However, more striking is the contrast between the cells treated with BNF for 2 hr and those treated with GA for 2 hr. In the GA-treated cells, the level of nuclear staining is reduced by approximately 70% (Table 1) and this change is consistent with the reduction in zfAHR2 protein observed by Western blotting (Fig. 5). The ability to observe ligand-mediated changes in the distribution of the zfAHR2 staining and reductions in the level of staining following treatment with BNF and GA validates the specificity of the zf-24 antibody.

Since a significant portion of the zfAHR2 pool appears to be nuclear under control culture conditions, it was of interest to determine whether the zfAHR2 was undergoing dynamic nucleocytoplasmic shuttling. To evaluate this process, ZFL cells were treated with leptomycin B (LMB) for 4 hr prior to fixation. LMB is an inhibitor of CRM-1-mediated nuclear export [43,44] and it is expected that a protein undergoing dynamic shuttling would accumulate in the nucleus if nuclear export were inhibited. Figure 6 shows that the staining for the zfAHR2 is reduced in the cytoplasm and increased in the nucleus (similar to cells treated with BNF for 2 hr) following 4 hr of LMB exposure (see Table 1). This result is consistent with a hypothesis that the zfAHR2 is shuttling between the nucleus and cytoplasm. Active nucleocytoplasmic shuttling of the mammalian AHR has recently been observed in several cell lines and the significance of this process to AHR-mediated signal transduction is currently under investigation ([9], unpublished results).

### 3.6. Conclusions and implications

Previous studies on the AHR signaling pathway in fish have focused primarily on the rainbow trout and *Fundulus heteroclitis* models. Many of these studies have used transient transfection of the respective fish AHRs into mammalian cell culture or studied the response of a few select cell lines following exposure to TCDD or other AHR ligands [45–49]. While many of these studies have produced important results with regard to establishing the presence of multiple AHR isoforms in fish, the analysis of changes in AHR protein concentration and its localization and interaction with other proteins has been difficult due to the lack of specific antibodies that could react with the endogenous AHR in the various model systems. Recently, much of the work on AHR signaling in fish has shifted toward the zebrafish model due to the better-defined developmental biology and ease of use compared to trout. Unfortunately, the inability to study the endogenous AHR in zebrafish has been a limitation.

The results presented in this report, demonstrate that a highly specific antibody has been developed that can detect *in vitro* expressed zfAHR2 as well as the endogenous zfAHR2 in ZFL cells. Importantly, the results show that the ZFL cell line is an appropriate model in which to study

the AHR signaling pathway and that the zfAHR2 is degraded via the 26S proteasome following ligand-dependent and -independent stimulation. These results suggest that zebrafish represent a non-mammalian model in which to study the degradation of the AHR and the attenuation of AHR-mediated signaling events. Interestingly, while the ligand-independent degradation of the zfAHR2 appeared to parallel results observed in mammalian systems with regard to the magnitude of zfAHR2 loss and the speed of the degradation events (Fig. 5), the ligand-mediated degradation of the zfAHR2, although very pronounced, did not appear to proceed at the same rate and to the same level as that observed in mammalian systems (Fig. 4). This suggests that there may be some important differences in fish that could provide novel information regarding the degradation process. Currently the 26S proteasome has not been isolated from zebrafish, but amino acid comparisons of mammalian and piscine AHRs reveal several differences with regard to the conservation of lysine residues. Lysines are necessary for ubiquitination of proteins targeted to the 26S proteasome [50]. Mammals have lysines in conserved locations throughout the entire AHR even in regions that have greatly reduced amino acid identity. Analysis of rainbow trout, fundulus, zebrafish and medaka show that while the lysines within the NH-terminal portion of the protein are conserved in location when compared to mammalian AHRs, fish are lacking some of the lysines found in the PAS and COOH-terminal portion of the protein. Since the precise lysines utilized in the ligand-mediated degradation of the AHR are currently unknown, continued study of the zfAHR2 and mammalian AHRs may provide important insight into the mechanism of ligand-dependent and -independent degradation of the AHR.

In summary, the studies in this report demonstrate the development of a highly specific antibody against the zfAHR2 that can detect the endogenous AHR protein in the ZFL cell line. Importantly, the results show that the zfAHR2 is a substrate for the 26S proteasome following both ligand-dependent and ligand-independent activation of the receptor protein. This is an important finding for a number of reasons. First, it shows that the mechanism of attenuation of the AHR signal transduction pathway is conserved between mammals and fish. Second, the results validate zebrafish as an appropriate model to investigate the consequence of AHR degradation and the domains of the protein required for this process. Lastly, it provides and novel model system in which to study protein ubiquitination and the proteasome. Future studies are aimed at evaluating the ability of the zf-24 to detect zfAHR2 in zebrafish and detailing the mechanism of zfAHR2 turnover.

## Acknowledgments

Special thanks to R. Tanguay who kindly supplied the zfAHR2 expression cDNAs and shared unpublished data. Jesal Popat is also acknowledged for technical assistance with some of the experiments. This work was supported in part by National Institute of Health grants ES-08980 and ES-10410 to R.S.P.

## References

[1] Belair CD, Peterson RE, Heideman W. Disruption of erythropoisis by dioxin in the zebrafish. Dev Dyn 2001;222:581–94.
[2] Teraoka H, Dong W, Ogawa S, Tsukiyama S, Okuhara Y, Niiyama M, Uneno N, Peterson RE, Hiraga T. 2,3,7,8-Tetrachlorodibenzo-*p*-dioxin toxicity in the zebrafish embryo: altered blood flow and impaired lower jaw development. Toxicol Sci 2002;65:192–9.
[3] Dong W, Teraoka H, Yamazaki K, Tsukiyama S, Imani S, Imagawa T, Stegeman JJ, Peterson RE, Hiraga T. 2,3,7,8-Tetrachlorodibenzo-*p*-dioxin toxicity in zebrafish embryo: local circulation failure in the dorsal midbrain is associated with increased apoptosis. Toxicol Sci 2002;69:191–201.
[4] Henry TR, Spitsbergen JM, Hornung MW, Abnet CC, Peterson RE. Early life stage toxicity of 2,3,7,8-tetrachlorodibenzo-*p*-dioxin in zebrafish (*Danio rerio*). Toxicol Appl Pharmacol 1997;142:56–68.
[5] Prasch AL, Teraoka H, Carney SA, Dong W, Hiraga T, Stegeman JJ, Heideman W, Peterson RE. Aryl hydrocarbon receptor 2 mediates 2,3,7,8-tetrachlorodibenzo-*p*-dioxin developmental toxicity in zebrafish. Toxicol Sci 2003;76:138–50.
[6] Tanguay RL, Abnet CC, Heideman W, Peterson RE. Cloning and characterization of the zebrafish (*Danio rerio*) aryl hydrocarbon receptor. Biochem Biophys Acta 1999;1444:35–48.
[7] Andreasen EA, Hahn ME, Heideman W, Peterson RE, Tanguay RL. The zebrafish (*Danio rerio*) aryl hydrocarbon receptor type I (zfAHR1) is a novel vertebrate receptor. Mol Pharmacol 2002;62:234–49.
[8] Hahn ME. Aryl hydrocarbon receptors: diversity and evolution. Chem-Biol Int 2002;141:131–60.
[9] Petrulis JR, Kusnadi A, Ramadoss P, Hollingshead B, Perdew GH. The hsp90 co-chaperone XAP2 alters importin β recognition of the bipartite nuclear localization signal of the Ah receptor and represses transcriptional activity. J Biol Chem 2003;278:2677–85.
[10] Petrulis JR, Perdew GH. The role of chaperone proteins in the aryl hydrocarbon receptor core complex. Chem Biol Interact 2002;141:25–40.
[11] Heid SE, Pollenz RS, Swanson HI. Role of heat shock protein 90 in mediating agonist-induced activation of the aryl hydrocarbon receptor. Mol Pharm 2000;57:82–92.
[12] Lees MJ, Whitelaw ML. Multiple roles of ligand in transforming the dioxin receptor to an active basic helix loop helix PAS transcription factor complex with the nuclear protein ARNT. Mol Cell Biol 1999;19:5811–22.
[13] Swanson HI. DNA binding and protein interactions of the AHR/ARNT heterodimer that facilitate gene activation. Chem-Biol Int 2002;141:63–76.
[14] Pollenz RS. The mechanism of AH receptor down regulation (degradation) and its impact on AH receptor mediated gene regulation. Chem-Biol Int 2002;141:41–62.
[15] Song Z, Pollenz RS. Ligand dependent and independent modulation of AH receptor localization, degradation, and gene regulation. Mol Pharmacol 2002;62:806–16.
[16] Davarinos N, Pollenz RS. Aryl hydrocarbon receptor imported into the nucleus following ligand binding is rapidly degraded via the cytoplasmic proteasome following nuclear export. J Biol Chem 1999;274:28708–15.
[17] Pollenz RS, Barbour ER. Analysis of the complex relationship between nuclear export and Ah receptor-mediated gene regulation. Mol Cell Biol 2000;20:6094–105.

[18] Song Z, Pollenz RS. Analysis of nuclear import of the Ah receptor. Mol Pharmacol 2003;63:597–606.
[19] Ma Q, Whitlock Jr JP. The AHR modulates the Hepa-1c1c7 cell cycle and differentiated state independently of dioxin. Mol Cell Biol 1996; 16:2144–50.
[20] Fernandez-Salguero P, Pineau T, Hilbert DM, McPhail T, Lee SS, Kimura S, Nebert DW, Rudikoff S, Ward JM, Gonzalez FJ. Immune system impairment and hepatic fibrosis in mice lacking the dioxin-binding Ah receptor. Science 1995;268:722–6.
[21] Hushka LJ, Williams JS, Greenlee WF. Characterization of 2,3,7,8-tetrachlorodibenzofuran-dependent suppression and AH receptor pathway gene expression in the developing mouse mammary gland. Toxicol Appl Pharmacol 1998;152:200–10.
[22] Peters JM, Narotsky MG, Elizondo G, Fernandez-Salguero PM, Gonzalez FJ, Abbott BD. Amelioration of TCDD-induced teratogenesis in the aryl hydrocarbon receptor (Ahr)-null mice. Toxicol Sci 1999;47:86–92.
[23] Schmidt JV, Su GH, Reddy JK, Simon MC, Bradfield CA. Characterization of a murine Ahr null allele: involvement of the Ah receptor in hepatic growth and development. Proc Natl Acad Sci USA 1996;93: 6731–6.
[24] Abbott BD, Schmid D, Pitt JE, Buckalew AR, Wood CR, Held GA, Diliberto JJ. Adverse reproductive outcomes in the transgenic Ah receptor-deficient mouse. Toxicol Appl Pharmacol 1999;155: 62–70.
[25] Heimler I, Trewin AL, Chaffin CL, Rawlins RG, Hutz RJ. Modulation of ovarian follicle maturation and effects on apoptotic cell death in Holtzman rats exposed to 2,3,7,8-tetrachlorodibenzo-*p*-dioxin (TCDD) in utero and lactationally. Reprod Toxicol 1998;12:69–73.
[26] Wolf CJ, Ostby JS, Gray LE. Gestational exposure to 2,3,7,8-tetrachlorodibenzo-*p*-dioxin (TCDD) severely alters reproductive function of female hamster offspring. Toxicol Sci 1999;51:259–64.
[27] Benedict JC, Lin TM, Loeffler IK, Peterson RE, Flaws JA. Physiological role of the aryl hydrocarbon receptor in mouse ovary development. Toxicol Sci 2000;56:382–8.
[28] Holmes JL, Pollenz RS. Determination of aryl hydrocarbon receptor nuclear translocator protein concentration and subcellular localization in hepatic and nonhepatic cell culture lines: development of quantitative western blotting protocols for calculation of aryl hydrocarbon receptor and aryl hydrocarbon receptor nuclear translocator protein in total cell lysates. Mol Pharmacol 1997;52:202–11.
[29] Pollenz RS, Sattler CA, Poland A. The aryl hydrocarbon receptor and aryl hydrocarbon receptor nuclear translocator protein show distinct subcellular localizations in Hepa 1c1c7 cells by immunofluorescence microscopy. Mol Pharmacol 1994;45:428–38.
[30] Pollenz RS, Sullivan HR, Holmes J, Necela B, Peterson RE. Isolation and expression of cDNAs from rainbow trout (*Oncorhynchus mykiss*) that encodes two novel basic-helix-loop-helix/PER-ARNT-SIM (bHLH/PAS) proteins with distinct functions in the presence of the aryl hydrocarbon receptor. J Biol Chem 1996;271:30886–96.
[31] Necela B, Pollenz RS. Functional analysis of activation and repression domains of the rainbow trout aryl hydrocarbon receptor nuclear translocator (rtARNT) protein isoforms. Biochem Pharmacol 1999; 57:1177–90.
[32] Necela B, Pollenz RS. Identification of a novel C-terminal domain involved in the negative function of rainbow trout Ah receptor nuclear translocator protein isoform a (rtARNTa) in Ah receptor-mediated signaling. Biochem Pharmacol 2001;62:307–18.
[33] Miranda CL, Collodi P, Zhao X, Barnes DW, Buhler DR. Regulation of cytochrome P450 expression in a novel liver cell line from zebrafish (*Brachydanio rerio*). Arch Biochem Biophys 1993;305:320–7.
[34] Collodi P, Miranda CL, Zhao X, Buhler DR, Barnes DW. Induction of zebrafish (*Brachydanio rerio*) P450 *in vivo* and in cell culture. Xenobiotica 1994;24:487–93.
[35] Ghosh C, Zhou YL, Collodi P. Derivation and characterization of a zebrafish liver cell line. Cell Biol Toxicol 1994;10:167–76.
[36] Ma Q, Baldwin KT. 2,3,7,8-Tetrachlorodibenzo-*p*-dioxin-induced degradation of aryl hydrocarbon receptor (AhR) by the ubiquitin-proteasome pathway. Role of the transcription activation and DNA binding of AhR. J Biol Chem 2000;275:8432–8.
[37] Roberts BJ, Whitelaw ML. Degradation of the basic-helix-loop-helix/Per-ARNT-Sim homology domain dioxin receptor via the ubiquitin/proteasome pathway. J Biol Chem 1999;274:36351–6.
[38] Grenert JP, Sullivan WP, Fadden P. The amino-terminal domain of heat shock protein 90 (hsp90) that binds geldanamycin is an ATP/ADP switch domain that regulates hsp90 conformation. J Biol Chem 1997; 272:23843–50.
[39] Whitesell L, Minmaugh EG, Costa BD, Meyers CE, Neckers LM. Inhibition of heat shock protein HSP90-pp60v-src heteroprotein complex formation by benzoquinone ansamycins: essential role for stress proteins in oncogenic transformation. Proc Natl Acad Sci USA 1994; 91:8324–8.
[40] Schulte TW, Blagosklonny MV, Ingui C, Neckers LM. Disruption of the Raf-1-Hsp90 molecular complex results in destabilization of Raf-1 and loss of Raf-1-Ras association. J Biol Chem 1995;261:24585–8.
[41] Chen H-S, Singh SS, Perdew GH. The Ah receptor is a sensitive target of geldanamycin-induced protein turnover. Arch Biochem Biophys 1997;348:190–8.
[42] Meyer BK, Petrulis JR, Perdew GH. Aryl hydrocarbon receptor levels are selectively modulated by the hsp90-associated immunophilin homolog XAP2. Cell Stress Chaperones 2000;5:243–54.
[43] Kudo N, Khochbin S, Nishi K, Kitano K, Yanagida M, Yoshida M, Horinouchi S. Molecular cloning and cell cycle-dependent expression of mammalian CRM1, a protein involved in nuclear export of proteins. J Biol Chem 1997;272:29742–51.
[44] Kudo N, Wolff B, Sekimoto T, Schreiner E, Yoneda Y, Yanagida M, Horinouchi S, Yoshida M. Leptomycin B inhibition of signal-mediated nuclear export by direct binding to CRM1. Exp Cell Res 1998;242: 540–7.
[45] Zabel EW, Pollenz RS, Peterson RE. Relative potencies of individual polychlorinated dibenzo-*p*-dioxin, dibenzofuran and biphenyl congeners and congener mixtures based on induction of cytochrome P4501A mRNA in a rainbow trout gonadal cell line (RTG-2). Environ Toxicol Chem 1996;15:2310–8.
[46] Pollenz RS, Necela B. Characterization of two continuous cell lines derived from *Oncorhynchus mykiss* for models of aryl-hydrocarbon-receptor-mediated signal transduction. Direct comparison to the mammalian hepa-1c1c7 cell line. Aquatic Toxicol 1998;41:31–49.
[47] Abnet CC, Tanguay RL, Hahn ME, Heideman W, Peterson RE. Two form of aryl hydrocarbon receptor type 2 in rainbow trout (*Oncorhynchus mykiss*): evidence for differential expression and enhancer specificity. J Biol Chem 1999;274:15159–66.
[48] Karcher SI, Powell WH, Hahn ME. Identification and functional characterization of two highly divergent aryl hydrocarbon receptors (AHR1 and AHR2) in the teleost *Fundulus heteroclitis*. J Biol Chem 1999;274:33814–24.
[49] Pollenz RS, Necela BN, Sojka K. Analysis of rainbow trout Ah-receptor isoforms in cell culture reveals conservation of function. Biochem Pharm 2002;64:49–60.
[50] Glickman MH, Ciechanover A. The ubiquitin-proteasome proteolytic pathway: destruction for the sake of construction. Phys. Rev. 2002:82; 373–428.